

# DETERMINATION OF CORROSION PARAMETERS FOR A CATHODIC REACTION COMPLICATED BY IR DROP EFFECT IN A FLOW SYSTEM

A. S. Yaro, and Q. J. Slaiman\*

Chemical Engineering Department – College of Engineering – University of Baghdad – Iraq

Chemical Engineering Department – College of Engineering – University of Saddam – Iraq

## ABSTRACT

In potential measurements, the ohmic drop commonly called "IR drop" is usually negligible at low current densities, but may be appreciable at high current densities due to the non-linear nature of current-potential relation that includes the effect of charge transfer, diffusion, and ohmic potential drop: In this investigation, experimental polarization studies of the corrosion parameters in an electrochemical flow cell of rectangular cross-section are made under deaerated = HCl solutions at a fixed  $Re 10^4$  in order to eliminate the effect of mass transfer, with temperature in the range (30-60°C) and acid concentration in the range (0.08-0.5 N) as variables. A theoretical cathodic model equation has been derived with IR-drop correction factor ( $\gamma$ ):

$$i_c = \gamma i_{corr} e^{\frac{2.303\Delta E}{bc}} \quad (1)$$

where

$$\gamma = \frac{1}{1 + \left( \frac{2.303R_c A}{bc} \right) i_{corr} e^{\frac{2.303\Delta E}{bc}}} \quad (2)$$

## INTRODUCTION

The effect of the electrolyte resistance and surface films known as IR-drop had not been given sufficient attention in corrosion studies. Stern and Geary<sup>[1]</sup> in their linear polarization technique renewed such attention which was followed by a discussion due to Oldham and Mansfeld<sup>[2]</sup>.

The neglect of this important experimental factor was due to or attributed to misunderstanding at that time between polarization resistance and the actual meaning of IR-drop. Besides that the uncompensated IR-drop in the vicinity of  $E_{corr}$ . Is considered insignificant.

Mansfeld<sup>[3]</sup>, discussed, in depth, the effect of uncompensated IR-drop on corrosion rate determination using polarization resistance measurements. It was shown that even in high conducting solutions involving high corrosion rates, the IR-drop although small, could not be disregarded.

Kajimoto et al<sup>[4]</sup> showed that large potential approximation method can not be used directly to

measure the corrosion rate of carbon steel in acid solutions, because of IR-drop.

Kelly<sup>[5]</sup>, in his study on commercially pure iron in 0.5 M N3804 saturated with H<sub>2</sub>, observed a departure from linearity in cathodic polarization curves for current densities > 10 mA/cm<sup>2</sup> and attributed the deviation from linearity to IR-drop. This assumption in fact, is consistent with Mansfeld finding that for high corrosion rates the IR-drop can not be disregarded even in highly conducting solutions.

## THEORY

The general equation of current/potential relationship for cathodic reaction experiencing the effect of diffusion control, activation control, and IR-drop effects as given by Devereux<sup>[6]</sup> is:

$$i_c = \left\{ 1 - \frac{i_c}{i_{lim}} \right\}^{m_c} e^{\frac{-(E-E_c^*)}{bc}} e^{-\frac{i_c A R_c}{bc}} \quad (3)$$

Equation (3) theoretically is identical to the equation<sup>[7]</sup>:

$$\eta^T = \eta^A + \eta^c + \eta^{IR} \quad (4)$$

Equation (3) is based on analysis of the cathodic polarization curve in a potential range far away from the effect of the reverse anodic reaction. When:

$$i_c \ll i_{lim}; i_c/i_{lim} \rightarrow 0 \quad i_c \leq i_{lim} \quad (5)$$

Thus, the term  $(1-i_c/i_{lim}) \rightarrow 1.0$  (i.e., no mass transfer effect). Realizing that the present experimental is carried out at  $(Re=10^4)$ . Accordingly equation (3) becomes:

$$i_c = e^{-\frac{(E-E_c^*)}{bc}} e^{-\frac{i_c AR_c}{bc}} \quad (6)$$

At  $E=E_{corr}$ ,  $i_c=i_{corr}$ ;  $IR \rightarrow 0$  (i.e., at relatively small current densities, IR drop becomes insignificant and can be neglected<sup>[8]</sup>).

Hence, equation (6) becomes:

$$i_{corr} = e^{-\frac{(E-E_c^*)}{bc}} \quad (7)$$

where  $E_c^*$  is a constant parameter, including both exchange current density and cathodic equilibrium potential of the reaction<sup>[8]</sup>, dividing equation (6) by equation (7) leads to:

$$\frac{i_c}{i_{corr}} = e^{\frac{(E_{corr}-E)}{bc}} e^{-\frac{i_c AR_c}{bc}} \quad (8)$$

Defining  $E_{corr}-E=\Delta E$ ;  $bc=2.303RT/\alpha_c F$  (based on log). Equation (8) can be rewritten as:

$$\frac{i_c}{i_{corr}} = e^{\frac{2.303\Delta E}{bc}} e^{-\frac{2.303i_c AR_c}{bc}} \quad (9)$$

linearizing the 2<sup>nd</sup> term on the RHS of equation (9), using Taylor series expansion leads to:

$$e^{-\frac{2.303i_c AR_c}{bc}} = 1 - \frac{2.303i_c AR_c}{bc} \quad (10)$$

Substituting equation (10) in equation (9) and rearranging leads to the following equation:

$$i_c = \frac{bc i_{corr} e^{\frac{2.303\Delta E}{bc}}}{bc + 2.303 i_{corr} R_c A e^{\frac{2.303\Delta E}{bc}}} \quad (11)$$

Or

$$i_c = \gamma i_{corr} e^{\frac{2.303\Delta E}{bc}} \quad (12)$$

where  $\gamma$  is the IR-drop correction factor expressed mathematically as in Equation (2), and can be defined as the ratio of the applied cathodic current including IR-drop to the applied cathodic current due to the activation polarization only.

## EXPERIMENTAL WORK

The corrosion behavior of carbon steel in (0.08-0.5 N) deaerated HCl acid solutions, temperature range (30-60 °C) was investigated using potentiodynamic polarization technique in rectangular duct flow system at a fixed Reynolds No. ( $= Re$ ) =  $10^4$  in order to reduce almost completely concentration polarization effect of hydrogen evaluation reaction.

## Materials

### Electrodes

Carbon steel (type ASTM - 108) containing 0.1427% C, 0.0144% S, 0.042% Ni, 0.022% Cr, 0.752% Mn and 0.0267% Si, was used throughout the present investigation as flat electrodes, 14 cm long, 1 cm wide and 0.1 cm thick for potentiodynamic polarization studies.

### Solutions

Analar HCl acid (BDH Limited Poole, England) was used throughout the present experiments as a corrosion solution after dilution to the required normalities. The specifications of the acid used were as follows: Concentration (w/w) = 36%;  $H_2SO_4$  = 0.02% Specific gravity = 1.18; iron (Fe) = 0.0001% Non-volatile matter = 0.01%; lead (Pb) = 0.0005%, Free  $Cl^-$  = 0.0005%. High purity distilled water added to the concentrated acid in order to maintain the  $[H^+]$  ion concentration at the required normalities.

### Rectangular channel duct

A rectangular channel duct made of perspex was constructed for following the present investigation<sup>[9-11]</sup>. It was 0.6x4 cm in cross section (equivalent diameter,  $d_e = 1.0435$  cm) and 1.0 m long. The duct consists of three sections: (1) The upstream section 48 cm long in order to obtain a fully developed flow<sup>[10,12]</sup>. (2) Test section 20 cm long. (3) Down stream section 27 cm long in order to avoid disturbances at the outlet<sup>[13]</sup>.

The rectangular channel duct was mounted with wider surface horizontally.

### Electrochemical corrosion cell

The corrosion cell consisted of working, counter and reference electrodes. The working electrode was (14x1 cm) carbon steel flat specimen, 0.1 cm thick. The electrode length ( $L/d_e > 10$ ) was envisaged sufficient to assume fully developed mass transfer conditions<sup>[14,16]</sup>. The width of channel was chosen based on Diessler and Taylor<sup>[16]</sup>, work to avoid any side effect (i.e., side effects calculated from velocity profiles in non circular channels were found to be the important only for about 10% of the channel width nearest the vertical side walls). The electrodes were set flush to the center of the perspex decks with epoxy resin. A hole of (1 mm) diameter was drilled in the duct (1 mm) from the edge of the electrode and halfway along its length. A glass tube was fixed centrally through the drilled hole, and connected by a rubber tube to a saturated calomel reference electrode reservoir.

The platinum counter electrode, 17 cm long by 1.5 cm in width was mounted longitudinal to the direction of flow and directly opposite to the working electrode, with the counter being on the upper side.

QVF glass pipes, valves, and fittings were used to complete the flow system shown in Fig. (1).

### Specimen preparation

Specimens were cleaned by washing with liquid soap and tap water followed by distilled water, degreased by analar benzene and acetone, then annealed in a vacuum at 600 °C for 1 hr, then furnace cooled under vacuum to room temperature. Before each test, specimen was abraded in sequence on emery paper grades, 220, 320, 400 and 600 under running tap water on METASERV HAND GRINDER TRAY (ENGLAND), washed with running tap water and

distilled water, dried, degreased and rinsed with benzene and acetone respectively. The specimen dimensions were measured with vernier then left to dry for 1 hr over silica-gel ready for use. It is important to mention that the

specimen before use was etched for 1 hr in 1 N HCl solution at 30°C to insure better reproducibility of experimental results.

### Procedure

After supplying 10 liters of test solution, circulation through the by-pass section was started (see Fig. (1)) while N<sub>3</sub> gas (> 99.99% purity) was injected through the distributor continuously for no less than two hours<sup>[13, 17,18]</sup>, valves leading to the corrosion cell duct were closed during this time. The metal electrode was placed in its position as explained previously. The duct was evacuated for two minutes to remove air inside the duct, then purged with N<sub>2</sub>, evacuated again for two minutes, then purged with N<sub>2</sub> continuously for two hours. When deaeration was complete, the three-way valve was closed and N<sub>2</sub> purging was stopped. When the required temperature was achieved the flow was adjusted at the desired rate. The corrosion potential and polarization measurements were carried out while N<sub>3</sub> injection was maintained through the distributor to preserve positive N<sub>3</sub> pressure during the test duration.

Investigation was carried out using the standard CORROSCRIPT POTENTIOSTAT (Tacussel, France).

The corrosion potential was measured every 2 minutes for the 1<sup>st</sup> 10 minutes at the beginning, then every 5 minutes for 1 hr, by a digital avometer type CONAR Model M-1400 until it reached steady state (i.e., the difference in measured values becomes  $< \pm 5$  mV). Then the potential was adjusted at - 700 mV (SCE) and allowed to vary potentiodynamically at a rate of 37.5 mV/min<sup>[19]</sup> until it reached a potential positive to the corrosion potential (i.e., 200 mV). Potential versus log current was recorded on x-y recorder model EpL-2B supplied by TACUSSOL. Each test was made twice, and if reproducibility was indoubt a third test was carried out.

## RESULTS AND DISCUSSION

Because environment is a fundamental part of the whole corrosion process, and it plays an important role in corrosion reactions, it is

extremely important to consider the potential difference across the electrolyte which is often referred to as the ohmic or IR-drop, and may be large if either the current or the resistance of the electrolyte is large.

A statistical experimentation called the central composite rotatable design technique, was used for planning the experiments of the present investigation. A total of (12) runs were carried out according to this technique as shown in Table (1).

Equation (11) as derived is used to determine numerically the unknowns,  $i_{corr}$ ,  $b_c$  and  $(R_c A)$  by deriving linear equations and solving them by the method of averages<sup>[21,22]</sup>. The program was written in Basic Language and a minimum of three data points were required. To compute the values of unknowns, (15) data points were used in the program spaced equally at 10 mV stalling from  $A E = 50$  mV

from  $E_{corr}$ .5 applied currents were taken from polarization curves recorded potentiodynamically.

The initial guesses were set to (0.15-0.25) mA/cm<sup>2</sup> for corrosion current density as expected or visualized from polarization curves recorded experimentally, 120 mV for cathodic Tafel slope ( $b_c$ ) which is well known theoretically, and a value of (10-50) ohm.cm<sup>2</sup> for IR-drop.

The three parameters,  $i_{corr}$ ,  $b_c$  and  $(R_c A)$  values computed by the above iterative method are shown in Table (2).

The individual percent error between the experimental and calculated applied currents were also calculated in order to evaluate the fitting of the experimental results as shown in Table (3) for deaerated acid solutions, as example.

Table (1) Operating conditions corresponding to general composite design in deaerated acid solutions

Run No.	Temperature (°C)		Acid Normality	
	X <sub>1</sub>	T	X <sub>2</sub>	N
1	-1	34	-1	0.14
2	+1	55	+1	0.14
3	-1	34	-1	0.43
4	+1	55	+1	0.43
5	-1.414	30	0	0.29
6	+1.414	60	0	0.29
7	0	45	-1.414	0.08
8	0	45	+1.414	0.5
9-12	0	45	0	0.29

\* Center point is repeated 3-5 times to assess experimental reproducibility.

Table (2) Corrosion current density,  $b_c$  &  $R_c A$  in deaerated acid solutions obtained by iterative method ( $Re=10000$ , 2-variables experiments)

Run No.	$b_c$ (mV)	$i_{corr}$ mA/cm <sup>2</sup>	$R_c A$ ohm.cm <sup>2</sup>
1	138	0.11	54.3
2	114	0.25	12.42
3	136	0.16	21.42
4	126	0.54	8.62
5	123	0.14	10.64
6	122	0.47	9.03
7	122	0.33	10.77
8	124	0.20	10.77
9	135	0.24	9.25
10	133	0.31	7.90
11	142	0.29	7.74
12	114	0.22	10.34

Table (3) Individual percent error between the experimental and calculated applied current densities

T = 34°C (Coded = -1), N = 0.14 (Coded = -1), $b_c = 138$ ; and $i_{corr} = 0.11$ ; R = 54.3				
$\Delta E$ (mV)	$i_c$ (mA/cm <sup>2</sup> ) Exp.	$i_c$ (mA/cm <sup>2</sup> ) Calc.	((( $i_c$ ) <sub>exp.</sub> - ( $i_c$ ) <sub>calc.</sub> ) / ( $i_c$ ) <sub>exp.</sub> ) 100	
50	0.1905	0.1702	10.65	
60	0.2291	0.2355	-2.8	
70	0.2630	0.2679	-1.86	
80	0.3020	0.3031	-0.36	
90	0.3467	0.3412	1.58	
100	0.3802	0.3817	-0.39	
110	0.4169	0.4243	-1.77	
120	0.4677	0.4687	-0.21	
130	0.5012	0.5141	-2.54	
140	0.5495	0.5600	-1.9	
150	0.6026	0.6059	-0.55	
160	0.6310	0.6511	-3.18	
170	0.6918	0.6948	-0.43	
180	0.7244	0.7368	-1.7	
190	0.7586	0.7764	-2.3	

T = 55°C (Coded = +1), N = 0.14 (Coded = -1), $b_c = 114$ ; and $i_{corr} = 0.11$ ; R = 12.42				
$\Delta E$ (mV)	$i_c$ (mA/cm <sup>2</sup> ) Exp.	$i_c$ (mA/cm <sup>2</sup> ) Calc.	((( $i_c$ ) <sub>exp.</sub> - ( $i_c$ ) <sub>calc.</sub> ) / ( $i_c$ ) <sub>exp.</sub> ) 100	
50	0.5495	0.5855	-6.55	
60	0.6918	0.6907	-0.275	
70	0.8318	0.8172	1.75	
80	0.9550	0.9562	-0.125	
90	1.1220	1.1106	1.02	
100	1.3183	1.2791	2.95	
110	1.4791	1.4608	1.23	
120	1.6596	1.6522	0.445	
130	1.8197	1.8503	-1.68	
140	1.9953	2.0513	-2.8	
150	2.1878	2.2511	-2.89	
160	2.3988	2.4458	-1.9	
170	2.6303	2.6317	-0.05	
180	2.8840	2.8061	2.70	
190	3.0199	2.9667	1.76	

Table (3) Cont.

T = 34°C (Coded = -1), N = 0.43 (Coded = +1), bc = 136; and $i_{corr} = 0.16$ ; R = 21.42			
$\Delta E$ (mV)	$i_c$ (mA/cm <sup>2</sup> ) Exp.	$i_c$ (mA/cm <sup>2</sup> ) Calc.	$\frac{((i_c)_{exp} - (i_c)_{calc}) / (i_c)_{exp} \cdot 100}{}$
50	0.3162	0.3286	-3.92
60	0.3802	0.3808	-0.16
70	0.4365	0.4399	-0.78
80	0.5248	0.5061	3.56
90	0.5754	0.5799	-0.78
100	0.6607	0.6612	-0.076
110	0.7586	0.7500	1.13
120	0.8318	0.8459	-1.7
130	0.9550	0.9483	0.70
140	1.0471	1.0562	-0.87
150	1.1482	1.1685	-1.8
160	1.2590	1.2837	-1.96
170	1.3804	1.4002	-1.43
180	1.5736	1.5164	-0.185
190	1.6596	1.6307	1.74

Table (2) shows that the cathodic Tafel slope values for hydrogen evolution reaction at different conditions in deaerated acid solutions range between (114-142) mV/sec, which are in good agreement with theoretical cathodic Tafel slope for HER of 118 mV.

The deviation from 118 mV<sup>[23]</sup>, may be ascribed to change in symmetry of energy barrier (i.e.,  $\alpha \neq 0.5$ )<sup>[24]</sup> and the higher temperatures presently investigated (3,0-60°C).

Felloni<sup>[25]</sup>, obtained values of be equal to 123 and 148 mV at pH = 0-1.0 in 1 N (HCl+NaCl). Kajimoto and Wolynce<sup>^</sup> obtained be values of 122 and 130 mV for corrosion of carbon steel in 1 N HCl and 1 N H<sub>2</sub>SO<sub>4</sub> respectively. Desia and Desia<sup>[26]</sup> mentioned be values of 125 and 110 mV for corrosion of mild steel in 1.0 and 6 N HCl acid respectively.

Experimental studies on the determination of IR-drop as corrosion parameter and its effect on the corrosion rate and Tafel slope are very limited in the literature especially in acid media. Kajimoto and Walynes<sup>[4]</sup>, applied the large potential approximation method of corrosion rate determination of carbon steel in acid solutions. They found a value of IR-drop of 0.56, and 0.3 ohm.cm<sup>2</sup> for corrosion of carbon steel in 1 N HCl and 1 N H<sub>2</sub>SO<sub>4</sub> respectively.

Recalling Equation (2)

$$\gamma = \frac{1}{1 + \left( \frac{2.303R_c A}{bc} \right) i_{corr} e^{bc}} \frac{2.303\Delta E}{bc} \quad (2)$$

$\gamma$  values were calculated from Equation (2) using the corrosion parameters,  $i_{corr}$ , be, and (AR<sub>c</sub>) obtained from iterative method and mentioned in Tables (2, and 3) at different  $\Delta E$  values and test conditions in deaerated acid solutions. The results are given in Table (4).

The  $\gamma$  values given in Table (4) indicate that a decrease in potential (i.e., as AE moves in the direction of E<sub>corr</sub>. Is associated with an increase in  $\gamma$  values.

This confirms corrosion parameters where it was assumed that IR-drop at E<sub>corr</sub>. is relatively small and negligible.

It is important to mention here that the data of  $\gamma$  versus  $\Delta E$  in Table (4) fit a straight line for all conditions studied with a correlation coefficient of (0.95-0.99) and an intercept on y-axis approaches unity (i.e., IR-drop at E<sub>corr</sub>. is relatively small and not significant).

The influence of IR-drop on the cathodic polarization curve is shown in Figs. (2, and 3) as an example after correcting the experimental curves using IR-drop correction factor,  $\gamma$ , as shown by Equation (12), and Tables (5) and (6):

$$(i_{app} / \gamma) = i_{corr} e^{bc} \frac{2.303\Delta E}{bc} \quad (12)$$

Table (4)  $\gamma$  values under experimental conditions in deaerated acid solutions (Re=10000)

$\Delta E$ (mV)	Test Conditions					
	T = 34°C N = 0.14	T = 55°C N = 0.14	T = 34°C N = 0.43	T = 55°C N = 0.43	T = 30°C N = 0.29	T = 60°C N = 0.29
50	0.8133	0.8531	0.8808	0.8250	0.9346	0.8293
60	0.7866	0.8259	0.8619	0.7970	0.9222	0.8009
70	0.7573	0.7950	0.8404	0.7658	0.9079	0.7691
80	0.7253	0.7601	0.8164	0.7315	0.8911	0.7339
90	0.6909	0.7213	0.7897	0.6941	0.8717	0.6954
100	0.6541	0.6790	0.7602	0.6540	0.8495	0.6541
110	0.6165	0.6335	0.7280	0.6116	0.8242	0.6102
120	0.5753	0.5855	0.6932	0.5674	0.7956	0.5645
130	0.5341	0.5357	0.6560	0.5221	0.7638	0.5177
140	0.4925	0.4853	0.6169	0.4765	0.7287	0.4705
150	0.4509	0.4352	0.5762	0.4312	0.6904	0.4239
160	0.4100	0.3863	0.5344	0.3870	0.6494	0.3786
170	0.3703	0.3391	0.4921	0.3447	0.6061	0.3353
180	0.3323	0.2959	0.4500	0.3047	0.5610	0.2946
190	0.2964	0.2557	0.4085	0.2674	0.5148	0.2570

$\Delta E$ (mV)	Test Conditions					
	T = 45°C N = 0.08	T = 45°C N = 0.5	T = 45°C N = 0.29	T = 45°C N = 0.29	T = 45°C N = 0.29	T = 45°C N = 0.29
50	0.8530	0.9094	0.9814	0.9096	0.9252	0.8880
60	0.8277	0.8930	0.89047	0.8944	0.9133	0.8663
70	0.7991	0.8741	0.8889	0.8771	0.8996	0.8411
80	0.7671	0.8523	0.8709	0.8573	0.8841	0.8122
90	0.7317	0.8276	0.8505	0.8350	0.8666	0.7794
100	0.6930	0.7997	0.8275	0.8100	0.8468	0.7427
110	0.6515	0.7686	0.8018	0.7821	0.8248	0.7023
120	0.6075	0.7342	0.7733	0.7514	0.8003	0.6584
130	0.5617	0.6968	0.7420	0.7179	0.7733	0.6117
140	0.5148	0.6565	0.7080	0.6818	0.7438	0.5628
150	0.4677	0.6139	0.6715	0.6435	0.7119	0.5126
160	0.4211	0.5694	0.6329	0.6031	0.6778	0.4622
170	0.3759	0.5238	0.5924	0.5614	0.6417	0.4125
180	0.3328	0.4778	0.5507	0.5187	0.6039	0.3646
190	0.2923	0.4321	0.5082	0.4760	0.5648	0.3192

Table (5) Corrected applied currents by IR-drop correction factor at 0.29N deaerated acid solution for different temperatures

$E_{corr}-E$ mV	30°C		45°C		60°C	
	$i_{app. exp.}$ mA/cm <sup>2</sup>	$i_{app. corr.}$ mA/cm <sup>2</sup>	$i_{app. exp.}$ mA/cm <sup>2</sup>	$i_{app. corr.}$ mA/cm <sup>2</sup>	$i_{app. exp.}$ mA/cm <sup>2</sup>	$i_{app. corr.}$ mA/cm <sup>2</sup>
50	0.3162	0.3383	0.5248	0.591	0.955	1.1516
60	0.389	0.4218	0.631	0.7284	1.1482	1.4336
70	0.4677	0.5151	0.7412	0.8812	1.3183	1.7082
80	0.5744	0.6446	0.8913	1.0974	1.5136	2.0624
90	0.6607	0.7579	1.0471	1.3435	1.7378	2.499
100	0.7586	0.893	1.2023	1.6188	1.9953	3.0505
110	0.912	1.1065	1.4454	2.0581	2.2387	3.6688
120	1.0471	1.3161	1.5849	2.4072	2.5119	4.4498
130	1.2023	1.5741	1.8197	2.9748	2.7542	5.32
140	1.3804	1.8943	2.0893	3.7123	3.0199	6.4185
150	1.5849	2.2956	2.2387	4.3673	3.3884	7.9934
160	1.7338	2.676	2.5119	5.0019	3.6308	9.59
170	1.9953	3.292	2.7542	6.6769	3.9811	11.8732
180	2.2909	4.0814	3.0903	8.4759	4.1687	14.1804
190	2.5119	4.8794	3.3113	10.3393	4.3652	16.9852

Table (6) Corrected applied currents by IR-drop correction factor at 45°C in different acid concentrations

$E_{corr}-E$ mV	0.08 N		0.29 N		0.5 N	
	$i_{app. exp.}$ mA/cm <sup>2</sup>	$i_{app. corr.}$ mA/cm <sup>2</sup>	$i_{app. exp.}$ mA/cm <sup>2</sup>	$i_{app. corr.}$ mA/cm <sup>2</sup>	$i_{app. exp.}$ mA/cm <sup>2</sup>	$i_{app. corr.}$ mA/cm <sup>2</sup>
50	0.6918	0.811	0.5248	0.591	0.4365	0.4799
60	0.8318	1.005	0.631	0.7284	0.5248	0.5877
70	1	1.2514	0.7412	0.8812	0.631	0.7219
80	1.1428	1.4968	0.8913	1.0974	0.7586	0.89
90	1.3183	1.8017	1.0471	1.3453	0.912	1.102
100	1.5736	2.1841	1.2023	1.6188	1.0715	1.3399
110	1.7378	2.6674	1.4454	2.0581	1.1749	1.5286
120	1.9055	3.1366	1.5849	2.4072	1.3183	1.7956
130	2.0893	3.7196	1.8197	2.9748	1.5136	2.1722
140	2.3988	4.6597	2.0893	3.7123	1.7378	2.6471
150	2.6303	5.6239	2.2387	4.3673	1.9055	3.1039
160	2.8184	6.6929	2.5119	5.4347	2.1878	3.8423
170	3.0199	8.0338	2.7542	6.6768	2.3988	4.5796
180	3.3113	9.9498	3.0903	8.4759	2.6303	5.505
190	3.5481	12.1386	3.3113	10.3737	2.9512	6.8299

Fig (2) shows that: (a) Within the potential range studied (i.e., from  $E_{corr}$  to higher cathodic potential levels), the HER increases as the temperature increases and also after using  $\gamma$  correction factor, (b) The IR-drop is more

pronounced at the higher temperature for the same acid concentration.

It can be concluded that the error in corrosion parameters determination without using correction for IR-drop is found to depend on the potential range of the data being evaluated, the error was found to increase as the cathodic curve is made more negative.

In Fig. (3), the reverse situation is observed at 45°C when the acid concentration increased from 0.08 to 0.5 N. The HER decreases experimentally and after correction, so it can be concluded that the IR-drop effect at 45 °C is approximately the same and is acid concentration independent.

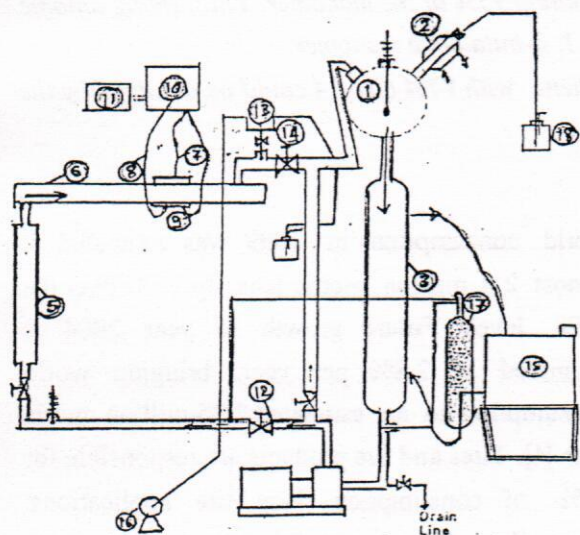
Finally Equation (11) derived theoretically for the cathodic polarization curve experiencing activation control (i.e., charge transfer) and IR-drop under present conditions is good and efficient tool for calculating the corrosion parameters when concentration polarization is not effective, hence it confirms that the IR-drop should be taken into consideration for accurate evaluation of corrosion parameters.

## REFERENCES

1. Stem, M. and Geary, A. L., J. Electrochem. Soc. 104, 56, 1957.
2. Mansfeld, F. and Oldham, K. B., Corrosion Sci., 11, 787, 1971.
3. Mansfeld, F., Corrosion, 32, 143, 1976.
4. Kajimoto, Z. P., Wolynes, S. and Chagas, H. C., Corrosion Sci., Vol. 25, No. 1, p.35-41, 1985.
5. Kelly, E. J., J. Electrochem. Soc. 112, 124, 1965.
6. Devereux, O. F., Corrosion, 35, 125, 1979.
7. West, J. M., "Electro Deposition and Corrosion Processes", V.N.R. Co., p. 5, 9, 55, 1971.
8. Yeum, K. S. and Devereux, O. F., Corrosion, Vol. 45, No. 6, 1989.
9. Pickett, D. J. and Ong, K. L., Electrochem. Acta, 19, 875, 1974.
10. Hubbard, D. W. and Lightfoot, B. N., I & BC Fundamentals, 15, 370, 1966.
11. Mizushima, T., Ogino, F., Oka, Y. and Fukuda, H., Int. J. Heat & Mass Transfer, 14, 1705, 1971.
12. Han, L. S., Trans. ASME 82 (J. App. Mech. 27), E 403, 1960.

13. Postleth Wake, J., Fiadzigba, E., and Aruliah, S., Corrosion, 34, 85, 1978.  
 14. Pickett, D. J. and Stanmore, B. R., J. Applied Electrochem., 2, 151, 1972.  
 15. Vanshow, P., Reiss, L. P. and Hanratty, T. J., AIChE Journal, 9, 362, 1963.  
 16. Deissler, R. G. and Taylor, M. F., NASA, TR4-31, 1959.  
 17. Slaiman, Q. J. M., and Al-Saaty, H. M., Proceeding 7<sup>th</sup> European symposium on Corrosion Inhibitors, p. 189, Ferrara, Italy, Seep. 1990.  
 18. Abdul-Masih, N. S., Ph.D. Thesis, University of Baghdad, 1990.  
 19. Mansfeld, F. and Kevding, M., Corrosion, 37, 545, 1981.

20. Box, G. B. P., and Hunter, J. C., Ann. Math., p. 195-241, Mar. 1957.  
 21. Scarborough, J. B., "Numerical Mathematical Analysis", p. 545-551, John Hopkins Press, Baltimor, 6<sup>th</sup> Ed. 1981.  
 22. Swinboume, E. S., "Analysis of Kinetic Data", p. 24-30, Applenton-Century-Croffts, New York, 1971.  
 23. Vetter, K., Electrochemical Kinetics, Academic Press, London, 1967.  
 24. Abdul-Azim, A. and Sanad, S. H., Corrosion Sci., 2, 337, 1972.  
 25. Felloni, L., Corrosion Sci., 8, 133, 1968.  
 26. Desai, M. N. and Desai M. B., Corrosion Sci., Vol 24, No. 8, p. 649-660, 1984.



- |                        |                      |
|------------------------|----------------------|
| 1- Reservoir           | 2- Condenser         |
| 3- Heat Exchanger      | 4- Pump              |
| 5- Rota meter          | 6- Flow Channel      |
| 7- Counter Electrode   | 8- Working Electrode |
| 9- Reference Electrode | 10- Potentiostat     |
| 11- Recorder           | 12- Valve            |
| 13- Three Way Valve    | 14- Valve            |
| 15- Water Bath         | 16- Vacuum Pump      |
| 17- Nitrogen Cylinder  | 18- Bubbling Flask   |

Fig. (1) Schematic diagram of flow apparatus for deaerated solutions

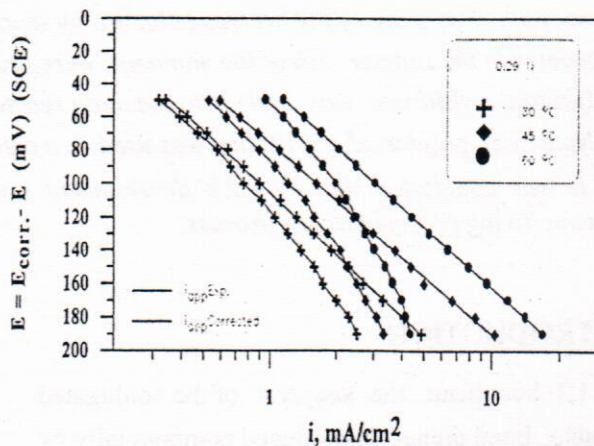


Fig. (2) Polarization results in deaerated HCl solutions at different temperatures corrected by  $\gamma$  method.

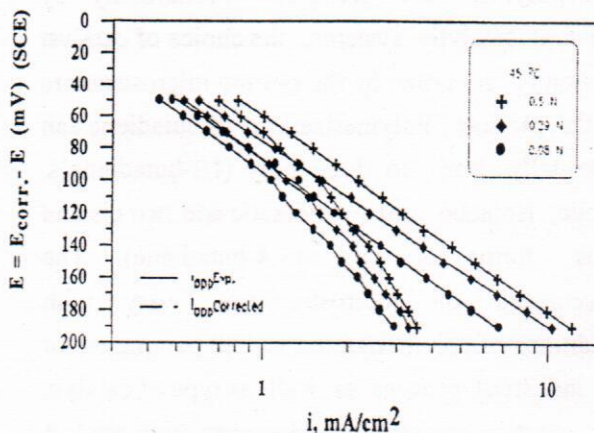


Fig. (3) Polarization results in different deaerated acid solutions at 45°C